Civil Engineering and Architecture 9(5A): 86-92, 2021 http://www.hrpub.org
DOI: 10.13189/cea.2021.091310

Experimental Investigation on Acoustic Emission Characteristics of Reinforced Concrete Beam Strengthened with CFRP

Soffian Noor Mat Saliah[1], Noorsuhada Md Nor[1,*], Khairul Nizam K.[1], Muhammad Ariffaizad M.M.[1], Mohd Subri Tahir[2]

[1]School of Civil Engineering, College of Engineering, Universiti Teknologi MARA, Cawangan Pulau Pinang, Pulau Pinang, Malaysia
[2]Department of Business Management, Universiti Teknologi MARA, Cawangan Pulau Pinang, Malaysia

Received October 16, 2020; Revised July 27, 2021; Accepted August 9, 2021

Cite This Paper in the following Citation Styles

***(a):** [1] Soffian Noor Mat Saliah, Noorsuhada Md Nor, Khairul Nizam K., Muhammad Ariffaizad M.M., Mohd Subri Tahir , "Experimental Investigation on Acoustic Emission Characteristics of Reinforced Concrete Beam Strengthened with CFRP," Civil Engineering and Architecture, Vol. 9, No. 5A, pp. 86 - 92, 2021. DOI: 10.13189/cea.2021.091310.*

***(b):** Soffian Noor Mat Saliah, Noorsuhada Md Nor, Khairul Nizam K., Muhammad Ariffaizad M.M., Mohd Subri Tahir (2021). Experimental Investigation on Acoustic Emission Characteristics of Reinforced Concrete Beam Strengthened with CFRP. Civil Engineering and Architecture, 9(5A), 86 - 92. DOI: 10.13189/cea.2021.091310.*

Abstract Reinforced concrete (RC) structures are generally subjected to increasing loads, age-related deterioration and design changes that affect the integrity of structures. Therefore, this paper presents an experimental investigation of a carbon fibre reinforced polymer (CFRP) reinforced RC beam under three-point loading. Acoustic emission (AE) was used to monitor the progression of damage. The loading, AE intensity and AE signal strength were analysed and discussed. The analyses were performed using the AE signal collected from CH6 and CH7. The result is that crack nucleation produces high signal intensity compared to other crack modes. Moreover, the intensity plots fit the identified crack modes when the beams were reinforced with CFRP. Therefore, AE can be used to evaluate the performance of the CFRP reinforced RC beam.

Keywords Acoustic Emission, Carbon Fibre Reinforced Polymer, Intensity Analysis, Strengthening

1. Introduction

Reinforced concrete (RC) is the most popular material used in construction industry all over the world. A major concern related to structure RC is the risk of deterioration due to ageing factors, changes in design, construction errors, or increasing load. Deterioration reduces the strength and integrity of RC structures. Much research has been conducted to reduce the deterioration of RC structure by reinforcing the structure with fibre reinforced polymer (FRP) laminates, such as carbon fibre reinforced polymer (CFRP). CFRP has been used to reinforce RC structures such as concrete arches [1], beam-column connections [2 - 4], beams [5 - 6], slabs [7 - 8] and columns [9]. Most researches have shown that the CFRP can increase the strength of RC structure. At the same time, the integrity of RC structure can be maintained even after failure [7]. The integrity of the CFRP reinforced structure RC is also related to the bonding and surface preparation of the concrete. Therefore, the bond and the effect of CFRP laminate on concrete surface were studied by Noorsuhada et al. [10]. They found that the type of surface preparation also affects the adhesion between the two materials in terms of tear strength. Although bonding plays an important role in the integrity of the concrete structure, a thorough investigation of the concrete structure reinforced with CFRP is also essential.

Most evaluations have been performed by visual observation, which is one of the nondestructive testing (NDT) methods. It is the simplest and least expensive technique to assess the integrity of the structure. Since integrity is closely related to crack development in the structure, visual observation offers inaccurate technique thus calling for further internal crack assessment if needed, because visual observation can only detect cracks noticeably appear on the surface. Hence, other NDT is required such as acoustic emission (AE) technique. Syamsiah et al. [11] used AE for investigation of the performance of mixture of plastic waste, wood dust, and rice husk. Ma et al. [12] used AE to monitor initial damage occurrence in the pre-damaged concrete column strengthened with CFRP at certain positions. They found that AE signals at early loading produced less energy for pre-damaged concrete columns strengthened with CFRP compared to intact concrete column strengthened with CFRP. Investigation carried out by Mohamad et al. [5] found that AE can identify two types of cracks in the concrete strengthened with CFRP known as tensile and shear cracks. Also, it is found that the integrity of the concrete structure strengthened with CRFP can be assessed using AE technique. However, the crack intensity of the RC structure strengthened with CFRP subjected to loading is still limited. This paper describes an experimental program to evaluate the beam reinforced with CFRP on the underside RC using the technique AE. The crack intensity for each crack mode at two channels is highlighted.

2. Methodology

2.1. Materials Preparation and Construction of RC Beams

RC beams with a width of 200 mm, a depth of 300 mm and a length of 1500 mm were prepared and laid out with concrete grade C40. The concrete mix was based on the weight percentages of cement, water, sand and coarse aggregates of 1.00, 0.43, 1.73 and 2.70 respectively. The compressive strength of the concrete was 56.87 MPa. In addition, 2T16 and 2T10 were used to reinforce the concrete at the tension and compression parts of the beam, respectively. The stirrups were designed as R8 - 175 mm c/c. Also, SikaWrap-231C type CFRP with tensile strength of 4900 N/mm^2 was used in this study. The epoxy resin used to laminate the CFRP to the concrete surface was Sikadur 330. The girder RC was reinforced with CFRP on the underside as per American Concrete Institute, ACI [13].

Prior to installing the CFRP, the surface preparation was carried out. The concrete surface was cleaned using compressed air. To laminate the CFRP onto the beam surface, epoxy resin type Sikadur 330 was used. The epoxy resin, Sikadur 330 of part A and part B, were mixed at a ratio of 4:1 by weight. The length of CFRP strip was cut to 1300 mm so that it was on the effective length of the beam. The CFRP strip was then cut longitudinally to width 200 mm using scissor. The CRFP was then laminated on the surface of the beam using epoxy resin.

2.2. Test Set-up, AE Monitoring and Analyses

Fig. 1 shows the structure of the beam for a three-point load with simultaneous monitoring by AE. A constant load rate of 0.02 kN/s was applied. The load was applied monotonically until the failure of the beam. AMSYS 6 with 34 dB preamplifier was used to monitor AE. Four VS75-V sensors were fixed on the beam surface as shown in Fig. 1 and designated as CH5, CH6, CH7 and CH8. Two sensors were fixed on the top of the beam 250 mm from the load point. Two more sensors were fixed on the side of the beam 300 mm away from the load point. A threshold of 40 dB was used when monitoring AE.

In this study, AE signal strength, load, crack pattern and intensity analysis were investigated and discussed. The intensity analysis was based on the AE signals collected at CH6 and CH7 at each crack mode. It was then compared to the crack pattern observed on the beam surface during testing.

3. Results and Discussion

3.1. AE Signal Strength, Load and Crack Modes of the Beam

Seven cracking modes were identified and designated as CM1, CM2, CM3, CM4, CM6 and CM7 for the CFRP reinforced beams at the bottom when subjected to monotonic loading to failure. Fig. 2 shows the relationship between the signal strength, load and time. The maximum load, P_{max}, of this beam was 258.66 kN. Fig. 3 shows the crack mapped on the beam surface. The CM1 crack was identified when a peak of high AE signal was detected during visual AE. However, no crack was visually observed on the beam surface when the beam was loaded with 31.67 kN, as shown in Fig. 3a. A high AE signal strength of 14800 nVs, as shown in Fig. 3, was detected when the load reached 12.27% of P_{max} at time 199 s, indicating the formation of CM1. The signal strength was recorded at CH6. Md Nor et al. [14] found that higher signal strength is developed during the early onset of the crack. This is also attributed to the stress concentration which is closely related to the presence and formation of the primary tensile crack.

As the load increased continuously to 60.85 kN (23.53% of Pmax), CM2, the first flexural crack, was visually observed. The crack occurred 850 mm from the left edge of the beam, as shown in Fig. 3b. It produced signal strength of 9730 nVs, lower than that of CM1. It was obtained from the wave emitted and collected by CH7 due to the amplification effect by the CFRP at the bottom of the beam, which reduced the energy dissipation of the concrete. More new flexural cracks appeared when the load was continuously increased, as shown in Fig. 3c. The CM3, flexural cracks were located when a load of 93.28 kN was reached at time 358 s and occurred at 36.06% of Pmax. New cracks occurred at 650 mm, 720 mm, 870 mm and 1100 mm from the left edge of the beam. The low signal strength was produced with the value of 4330 nVs at CH7.

For CM4, shear cracks were noticed on the beam surface as shown in Fig. 3d when the load of 123.20 kN or 47.63% of the P_{max} was subjected to the beam. It occurred at 467 s. Most of cracks propagated from the tip of the previous cracks. The signal strength was captured by CH7. It is found that no delamination of CFRP, CM4 occurred. It is associated with good surface preparation and mixing of the epoxy resin for lamination which produced good bonding between the CFRP and concrete surface. Hence, it gave high integrity to the beam. For CM5, plate and debonding between the concrete and the CFRP were noticed when the load of 222.71 kN or 86.10% of the P_{max} was subjected to the beam. The CM5 induced the high signal strength of 3880 nVs compared to CM4.

Illustration of the cracks on the side view can be seen in Fig. 4. The crack mode CM6 pattern is depicted in Fig. 3e which clearly shows that the CFRP is still in contact to the concrete even though the concrete cover has failed. It occurred due to good contact between concrete surface and the CFRP bonding. It is also related to the surface preparation prior to laminating the CFRP onto the concrete surface.

According to Teng et al. [15], concrete cover separation is closely related to CFRP plate-end debonding failure. Arduini et al. [16] and Chajes et al. [17] stated that the concrete surface preparation greatly influenced the ultimate bonding strength between the concrete and the CFRP. At the same time, the good contact between the concrete surface and the CFRP was obtained due to properly selected adhesive used to laminate the two materials. It was highlighted by Buyukoztruk et al. [18] that improper adhesive selection might promote debonding failure between the concrete and CFRP. They also stated that majority of debonding failure took place in the concrete substrate if good contact between CFRP and concrete was gained.

As the load increased continuously to 204.76 Kn (79.16% of P_{max}) at time 1590 s, the CM7, the reinforcement in the beam fractured. It produced a higher signal strength compared to the previous crack mode CM4 at 11000 nVs. The imaged crack pattern can be seen in Fig. 3f.

Figure 1. The beam setup in conjunction with AE monitoring

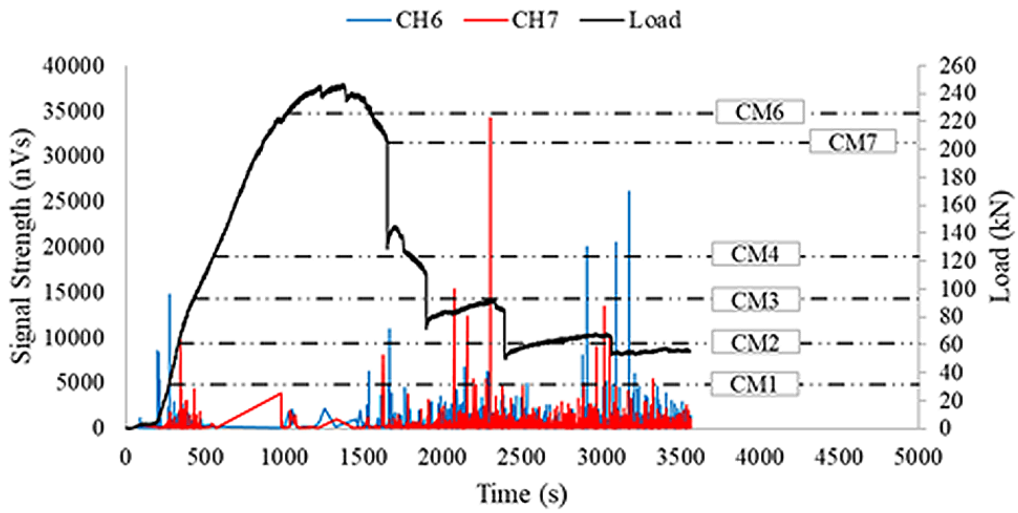

Figure 2. Relationship between signal strength and load and time

Due to the strengthening of CFRP, shear strength of the beam failed as depicted in Fig. 5. The CFRP produced high stress concentration at the end of the CFRP laminate. It was also stated by Buyukoztruk et al. [18] that the debonding in CFRP strengthened members takes place in the vicinity of high stress concentration which are often associated with material discontinuities.

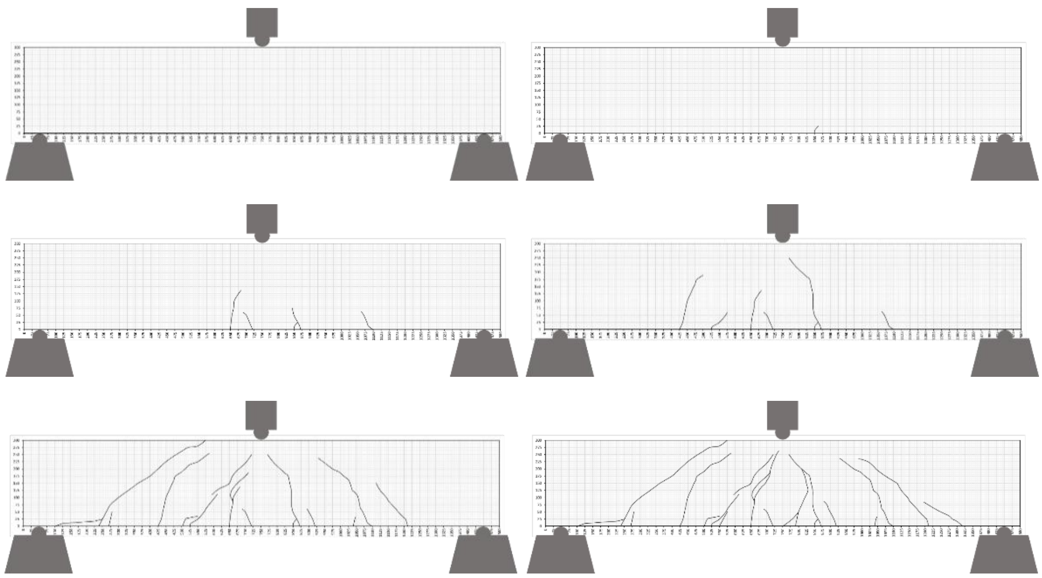

Figure 3. Illustration of the crack mapped on the beam surface a) CM1, b) CM2, c) CM3, d) CM4, e) CM6 and f) CM7

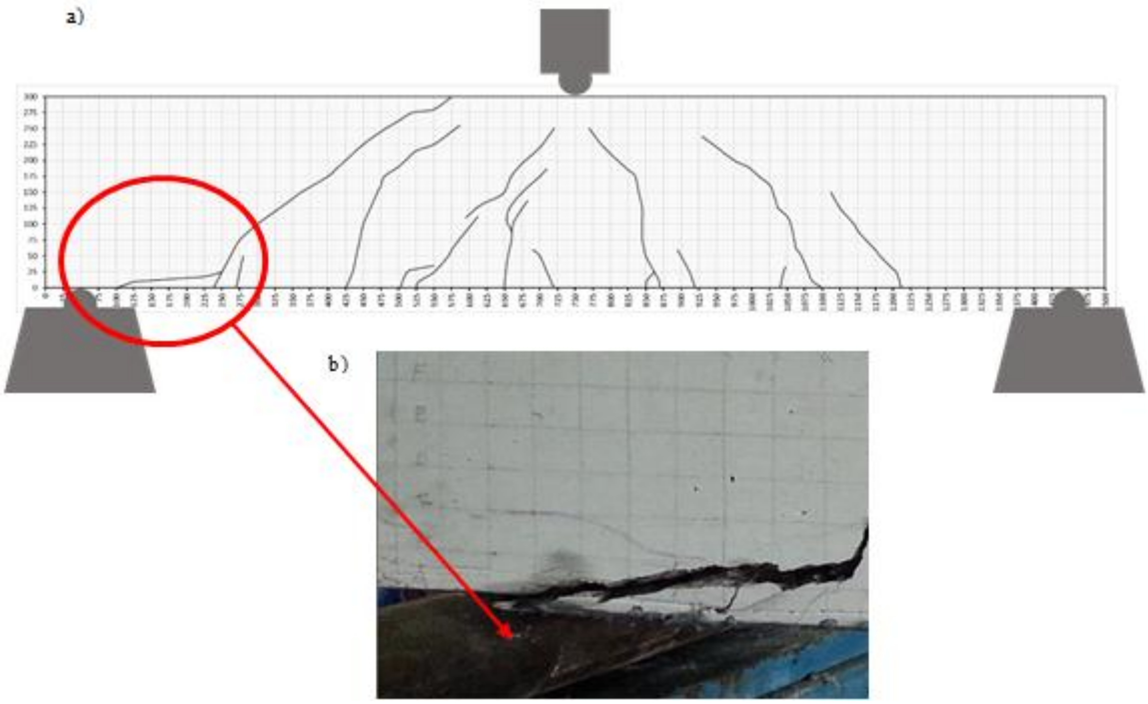

Figure 4 **a)** Crack pattern of the beam for crack mode plate and debonding **b)** Enlargement of the crack at support

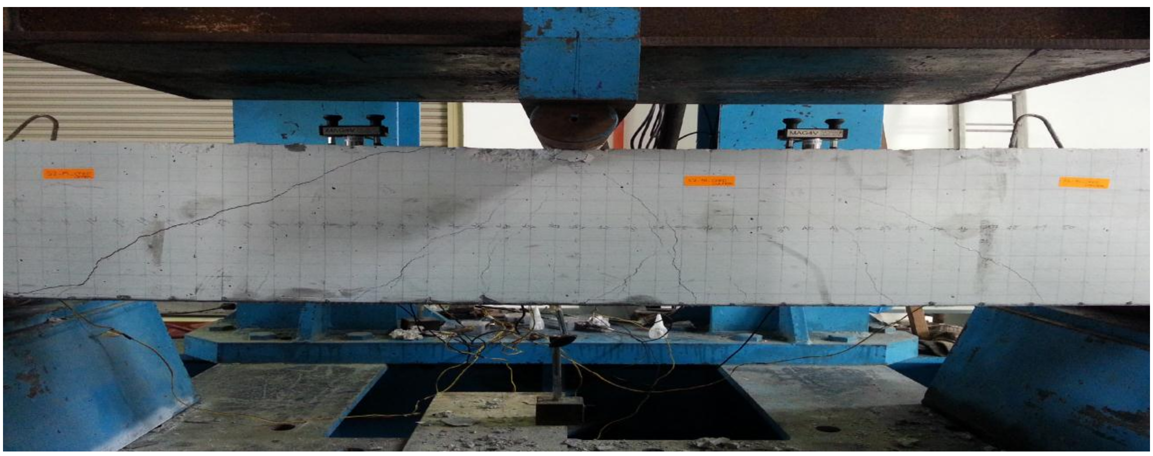

Figure 5. Crack pattern of the beam at failure

3.2. Crack Intensity of the Beam at CH6 and CH7

Fig. 6 shows the intensity of the crack zones for the beam at CM1 (M1). Since no crack occurred on the beam surface, the intensity crack zone plot shows that the beam is located in zone A. As the load increased and CM2 (M2) occurred, the intensity plot is in Zone B and Zone A is at CH6 and CH7, respectively. Although no crack can be visually seen under CH6, the intensity zone shows that the beam has a small crack, which means that the beam needs further investigation. Since the intensity analysis is closely related to the signal strength or energy of AE, the visible crack does not seem to produce a high energy that could be detected by CH7 compared to CH6. In general, the sensor closest to the crack would detect more energy than the sensor farthest away, which is closely related to the timing of the arrival of the AE wave at the sensor. Referring to the crack pattern in CM3 (M3), the intensity crack zone for CM2 derived from CH6 can predict the occurrence of an impending crack in the beam. Therefore, the intensity crack zone in CM2 can be used to predict the beam derived intensity zone when the load is increased to 93.28 kN. As Noorsuhada [19] states, intensity analysis can be used to predict the impending crack in the beam when it is subjected to load.

When the CM3 (M3) appeared on the beam surface, the plots in the intensity crack in Fig. 6 established that the CFRP-reinforced beam is located in Zone C and Zone B at CH6 and CH7, respectively. Looking at the crack pattern, it is found that the crack under CH6 forms and propagates much more than other cracks under CH7. The crack under

CH6 propagates almost in the middle of the beam. If the statement of McCormac and Nelson [20] is considered, the crack occurs beyond the neutral axis, which means that the rebars have yielded. This resulted in a high stress concentration in the beam. In this context, Zone C means that the beam experiences an intermediate damage that requires a follow-up evaluation.

When the load is increased to 123.20 kN, CM4 (M4) is identified. Further new cracks have developed and can be observed on the surface of the beam. Due to the presence of this crack, the AE intensity plot collected from CH6 and CH7 falls in Zone D. Zone D indicates a significant defect in the beam that requires a follow-up evaluation. Further cracks are visually observed under CH6 and CH7 when the load was increased to 222.71 kN. At this point, the concrete at the slab end of the CFRP was softened and designated as CM6 (M6). In this cracking mode, the AE intensity plot collected at CH6 and CH7 falls in Zone E. Zone E means that the beam reinforced with CFRP has a larger defect. In a real situation, the beam must be shut down immediately and the condition of the beam must be monitored in general. In this girder, a high stress concentration occurred at the plate end of the CFRP system. At this stage, the CFRP system can no longer support the applied load, and detachment of the plate end occurs. It is found that the failure of the CFRP system occurred after the occurrence of a shear crack. At the same time, the beam is still capable of resisting the applied load. As described in ACI 440.2R-02 [21], losses of the CFRP system do not lead to failure in the component.

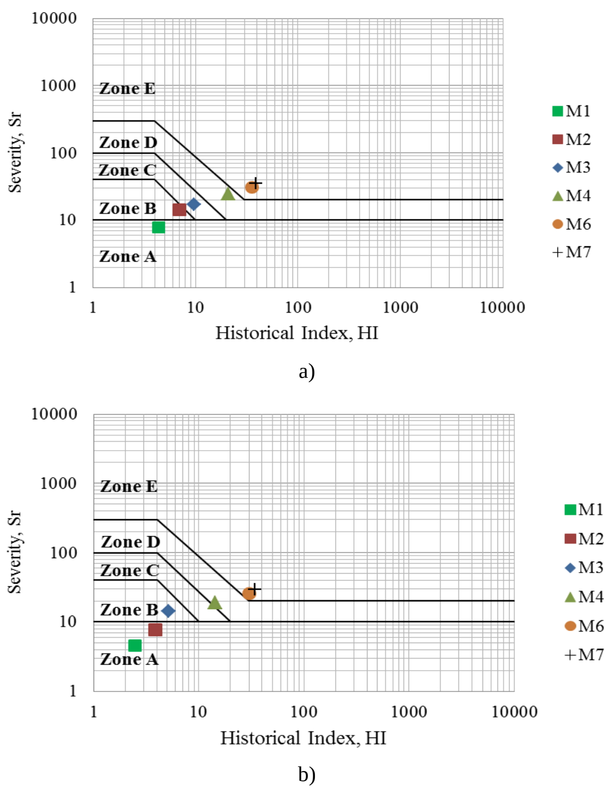

Figure 6. The intensity zone taken at a) CH6 b) CH7

4. Conclusions

In this study, the damage of the CFRP reinforced beam is evaluated using acoustic emission method. Six crack modes were identified namely CM1, CM2, CM3, CM4, CM6 and CM7. High signal intensity was observed in nucleation of crack CM1 due to higher stress concentration compared to other crack modes. From the intensity analysis, it can be concluded that as the stress increases, the crack mode also increases from no crack to failure. The plots in the intensity crack zones also increase from Zone A to Zone E for both CH6 and CH7. In summary, the intensity plots correspond well with the identified crack modes when the beam is reinforced with CFRP.

Acknowledgments

The authors thank the Faculty of Civil Engineering, Universiti Teknologi MARA (UiTM), Cawangan Pulau Pinang for providing the financial support in terms of materials allocation for this research. The authors would also like to thank the ICU JPM for the fee payment of this paper (100-IRMI/GOV 16/6/2 (001/2017). The authors would also like to acknowledge all assistant engineers who were involved in this research.

REFERENCES

[1] X. Zhang, P. Wang, M. Jiang, H. Fan, J. Zhou, W. Li, L. Dong, H. Chen, F. Jin. CFRP strengthening reinforced concrete arches: Strengthening methods and experimental studies, Composite Structures, Vol. 131, 852–867, 2015.

[2] E. Esmaeeli, J. A. O. Barros, J. Sena-Cruz, L. Fasan, F. Raimondo, L. Prizzi, J. Melo, H. Varum. Retrofitting of interior RC beam–column joints using CFRP strengthened SHCC: Cast-in-place solution, Composites Structures, Vol. 122, 456 – 467, 2015.

[3] M.N. Noorsuhada, M.S. Soffian Noor, M. Muhammad Zakaria, I. Azmi, A.M. Jalilluddin, T. Aqil Syafeeq, A.G. Kay Dora. Structural health monitoring of reinforced concrete beam-column joint using acoustic emission technique, International Journal of Advances in Science Engineering and Technology, Vol. 5, 50 – 55, 2017.

[4] W.T. Lee, Y.J. Chiou, M.H. Shih. Reinforced concrete beam-column joint strengthened with carbon fibre reinforced polymer, Composite Structures, Vol. 92, 48 – 60, 2010.

[5] M.Z. Mohamad, N. Md Nor, W.N.A. Wan Ahmad. Average frequency – RA value for reinforced concrete beam strengthened with carbon fibre sheet, MATEC Web of Conferences, Vol. 47, 1 – 6, 2016.

[6] A.N. Nayak, A. Kumari, R.B. Swain. Strengthening of RC beams using externally bonded fibre reinforced polymer composites, Structures, Vol. 14, 137–152, 2007.

[7] B. Abdul-Salam, A. S. Farghaly, B. Benmokrane. Mechanisms of shear resistance of one-way concrete slabs reinforced with FRP bars, Construction and Building Materials, Vol. 127, 959-970, 2016.

[8] G. Balamurugan, T.S. Viswanathan. Evaluation of the Effects of Orientation and Coverage Areas of FRP Lamination Bonded with Two-Way RC Slabs – A Modular Approach. Civil Engineering and Architecture, Vol. 8, No. 4, pp. 706 - 713, 2020. DOI: 10.13189/cea.2020.080432.

[9] C. Dundar, D. Erturkmen, S. Tokgoz. Studies on carbon fibre polymer confined slender plain and steel fibre reinforced concrete columns, Engineering Structures, Vol. 102, 31 – 39, 2015.

[10] M.N. Noorsuhada, M.S. Soffian Noor, A.M. Siti Norfahanim, M.H. Mohd Hisbany, M. Norfaridah. Acoustic emission signals of pull-off test for concrete slab strengthened with CFRP using various surface preparations, Key Engineering Materials, Vol. 821, 479 – 485, 2019.

[11] N. R. Syamsiyah , D. Mutiari , Y. Arsandrie , Suharyani , S. A. Himmah. Acoustic Performance from a Mixture of Plastic Waste, Wood Dust, and Rice Husk. Civil Engineering and Architecture, Vol. 8, No. 4, pp. 490 - 499, 2020. DOI: 10.13189/cea.2020.080412.

[12] G. Ma, H. Li, Z. Duan. Repair effects and acoustic emission technique-based fracture evaluation for predamaged concrete columns confined with fibre-reinforced polymers, Journal of Composites for Construction, Vol. 16, 626 – 639, 2012.

[13] ACI. Structural crack repair by epoxy injection in Concrete Repair Manual, 3rd Edition, edited by American Concrete Institute and International Concrete Repair Institute, 951 – 956, 2000.

[14] N. Md Nor, A. Ibrahim, N. Muhamad Bunnori, H. Mohd Saman, S.N. Mat Saliah, S. Shahidan. Diagnostic of fatigue damage severity on reinforced concrete beam using acoustic emission Technique, Engineering Failure Analysis, Vol. 41, 1-9, 2014.

[15] J.G. Teng, J.F. Chen, S. T. Smith, L. Lam. FRP-strengthened RC structures, Wiley, Technology & Engineering, 2002.

[16] M. Arduini, A. Nanni. Behaviour of precracked RC beams strengthened with carbon FRP sheets, Journal of composites for construction, ASCE, Vol. 1, 63-70, 1997.

[17] M.J. Chajes, W.W. Finch, T.F. Januszke, T.A. Thomson. Bond and force transfer of composite material plate bonded to concrete, ACI Structural Journal, Vol. 93, 208 – 217, 1996.

[18] O. Buyukozturk, O. Gunes, E. Karaca. Progress on understanding debonding problems in reinforced concrete and steel members strengthened using FRP composites, Construction and Building Materials, Vol. 18, 9 – 19, 2004.

[19] M.N. Noorsuhada. Structural health monitoring through acoustic emission, in Eco-Efficient Repair and Rehabilitation of Concrete Infrastructures, F. Pacheco-Torgal, Robert E. Melchers, Xianming Shi, Nele De Belie, Kim Van Tittelboom, and Andrés Sáez, Woodhead Publishing Series in Civil and Structural Engineering, 123-146, 2018.

[20] J.C. McCormac, J.K. Nelson. Design of reinforced concrete ACI 318-05 Code edition, ACI, 2006.

[21] ACI 440.2R – 02. Guide for design and construction of externally bonded FRP systems for strengthening concrete structures, American Concrete Institute, 2002.